ORIGINAL ARTICLE

gebiology | WILEY

Biogeochemical and physical controls on methane fluxes from two ferruginous meromictic lakes

Nicholas Lambrecht[1] (iD) | Sergei Katsev[2,3] | Chad Wittkop[4] | Steven J. Hall[5] |
Cody S. Sheik[3,6] | Aude Picard[7] | Mojtaba Fakhraee[3] | Elizabeth D. Swanner[1]

[1]Department of Geological and Atmospheric Sciences, Iowa State University, Ames, IA, USA

[2]Department of Physics, University of Minnesota Duluth, Duluth, MN, USA

[3]Large Lakes Observatory, University of Minnesota Duluth, Duluth, MN, USA

[4]Department of Chemistry and Geology, Minnesota State University, Mankato, MN, USA

[5]Department of Ecology, Evolution, and Organismal Biology, Iowa State University, Ames, IA, USA

[6]Department of Biology, University of Minnesota Duluth, Duluth, MN, USA

[7]School of Life Sciences, University of Nevada Las Vegas, Las Vegas, NV, USA

Correspondence
Nicholas Lambrecht, Department of Geological and Atmospheric Sciences, Iowa State University, 2337 Osborn Drive, Ames, IA 50011, USA.
Email: nlambrec@iastate.edu

Funding information
NSF, Grant/Award Number: EAR - 1660691, EAR - 1660761 and EAR - 1660873; Huron Mountain Wildlife Foundation; Canada Foundation for Innovation; Natural Sciences and Engineering Research Council of Canada; University of Saskatchewan; Government of Saskatchewan; Western Economic Diversification Canada; National Research Council Canada; Canadian Institutes of Health Research

Abstract

Meromictic lakes with anoxic bottom waters often have active methane cycles whereby methane is generally produced biogenically under anoxic conditions and oxidized in oxic surface waters prior to reaching the atmosphere. Lakes that contain dissolved ferrous iron in their deep waters (i.e., ferruginous) are rare, but valuable, as geochemical analogues of the conditions that dominated the Earth's oceans during the Precambrian when interactions between the iron and methane cycles could have shaped the greenhouse regulation of the planet's climate. Here, we explored controls on the methane fluxes from Brownie Lake and Canyon Lake, two ferruginous meromictic lakes that contain similar concentrations (max. >1 mM) of dissolved methane in their bottom waters. The order *Methanobacteriales* was the dominant methanogen detected in both lakes. At Brownie Lake, methanogen abundance, an increase in methane concentration with respect to depths closer to the sediment, and isotopic data suggest methanogenesis is an active process in the anoxic water column. At Canyon Lake, methanogenesis occurred primarily in the sediment. The most abundant aerobic methane-oxidizing bacteria present in both water columns were associated with the Gammaproteobacteria, with little evidence of anaerobic methane oxidizing organisms being present or active. Direct measurements at the surface revealed a methane flux from Brownie Lake that was two orders of magnitude greater than the flux from Canyon Lake. Comparison of measured versus calculated turbulent diffusive fluxes indicates that most of the methane flux at Brownie Lake was non-diffusive. Although the turbulent diffusive methane flux at Canyon Lake was attenuated by methane oxidizing bacteria, dissolved methane was detected in the epilimnion, suggestive of lateral transport of methane from littoral sediments. These results highlight the importance of direct measurements in estimating the total methane flux from water columns, and that non-diffusive transport of methane may be important to consider from other ferruginous systems.

KEYWORDS
ferruginous, lakes, meromictic, methane flux

1 | INTRODUCTION

Ferruginous (Fe-rich and anoxic) lakes that are meromictic (i.e., permanently stratified with respect to salinity) have been noted for their active CH_4 cycles, which includes the biological production of CH_4 in the anoxic sediment, and diffusion of CH_4 into the overlying water column where oxidation occurs (although, see Pasche et al. (2011) for alternative methanogenic pathways in volcanic lakes such as the reduction of geogenic CO_2). Slow vertical mixing and anoxic bottom waters that are depleted of electron acceptors (e.g., NO_3^- and SO_4^{2-}) lead to the accumulation of CH_4 in the water column.

Methane production rates under ferruginous conditions depend on the importance of methanogenesis relative to other organic carbon mineralization pathways, such as SO_4^{2-} and Fe(III) reduction. Thermodynamic considerations suggest the presence of Fe(III)-(hydr)oxides should promote Fe(III) reduction and preclude methanogenesis (Reeburgh, 2007). This is due to the relative energy microbes yield from Fe(III) reduction coupled to organic matter oxidation, which can be 10s of times more than the energy yielded by methanogenesis (Lovley & Chapelle, 1995). However, in ferruginous settings at circumneutral pH, Fe(II) is several orders of magnitude more soluble than Fe(III) (Thamdrup, 2011) and can sorb to the surfaces of Fe(III)-(hydr)oxides that may form at an oxic–anoxic boundary. This interaction renders the Fe(III)-(hydr)oxides less accessible to Fe(III)-reducing microbes (Roden & Urrutia, 1999, 2002).

In general, archaea mediate the production of CH_4 through methanogenesis, and CH_4 production in lakes usually occurs in the sediments (Rudd & Hamilton, 1978). The oxidation of CH_4 in lakes has largely been noted to occur at the oxic–anoxic boundary by aerobic methane-oxidizing bacteria (MOB; Hanson and Hanson, 1996), with fewer observations of anaerobic oxidation of methane (AOM) by anaerobic methanotrophic archaea (ANME) (e.g., Eller, Känel, & Krüger, 2005; Schubert et al., 2011). To date, the microbial cycling of CH_4 has been investigated in only a handful of ferruginous meromictic lakes, including Lake La Cruz, Lake Matano, Lake Svetloe, Woods Lake, and Lake Pavin (Biderre-Petit et al., 2011; Crowe et al., 2011; Dupuis, Sprague, Docherty, & Koretsky, 2019; Oswald, Jegge, et al., 2016a; Savvichev et al., 2017).

Despite the permanently high CH_4 reservoir in ferruginous meromictic lakes, CH_4 fluxes to the atmosphere are estimated to be low based on vertical reaction-transport modeling of water column CH_4 concentrations, which is biased toward turbulent diffusion as a transport mechanism. In one instance at Lake La Cruz, the aerobic MOB are suggested to mitigate all CH_4 emissions (Oswald, Milucka, et al., 2016b). In other lakes (e.g., Kabuno Bay of Lake Kivu, Lake Pavin, and Lake Matano), the depth of the water columns allows for oxidation of diffused CH_4 before significant portions can reach the atmosphere (Borges, Abril, Delille, Descy, & Darchambeau, 2011; Lopes et al., 2011; Sturm et al., 2018). In all cases, the CH_4 fluxes in these lakes are estimated to be lower compared to the lacustrine global average CH_4 flux (0.11 mmol m^{-2} hr^{-1}; Aselmann & Crutzen, 1989).

Ferruginous meromictic lakes can serve as analogs for Precambrian oceans, considering the accumulating evidence for pervasive ferruginous conditions below the mixed layer throughout much of Earth's history (Poulton & Canfield, 2011). Understanding factors that control CH_4 cycling from ferruginous systems can help discern how carbon was cycled under the geochemical conditions of early Earth. The focus on CH_4 extends out of the water column as it is one of the main gases thought to have regulated early Earth climate in the Archean. Paleoatmospheric modeling suggests that CH_4 was an important greenhouse gas, in addition to CO_2, that warmed Earth during the lower solar luminosity experienced in the Archean Eon (see Olson, Schwieterman, Reinhard, & Lyons, 2018 and references therein). As soon as methanogenesis evolved ~3.5 Ga (Ueno, Yamada, Yoshida, Maruyama, & Isozaki, 2006; Wolfe & Fournier, 2018), CH_4 could begin to accumulate in the reduced Archean atmosphere. In the absence of O_2, CH_4 is estimated to have reached a maximum of ~50× pre-industrial atmospheric levels (ca. 700 ppb; Etheridge, Steele, Francey, & Langenfelds, 1998) assuming pCO_2 near upper paleosol limits (Olson et al., 2018). After the "Great Oxidation Event" (ca. 2.4 Ga), pCH_4 in the atmosphere is estimated to have decreased to ~25 ppmv by the mid-Proterozoic due to microbial oxidation mitigating CH_4 fluxes (Fakhraee, Hancisse, Canfield, Crowe, & Katsev, 2019). Specifically, O_2-induced continental sulfide weathering introduced SO_4^{2-} to the oceans where SO_4^{2-}-based AOM diminished the flux of CH_4 drastically (Canfield, 2005; Catling, Claire, & Zahnle, 2007). Despite the introduction of SO_4^{2-}, ferruginous oceanic conditions persisted throughout most of Earth's history until the oxygenation of the deep oceans around 0.58 Ga (Canfield, Poulton, & Narbonne, 2007; Poulton & Canfield, 2011).

What ways can CH_4 be emitted from ferruginous meromictic lakes? Substantial CH_4 emission to the atmosphere via non-diffusive transport has been shown to occur out of water columns <100 m deep (McGinnis, Greinert, Artemov, Beaubien, & Wüest, 2006). Of the ferruginous meromictic lakes studied where the water columns are less than this threshold (Lake La Cruz and Lake Svetloe), the CH_4 flux has not been directly measured. Further, does the CH_4 flux differ among ferruginous meromictic lakes where a disparity in maximum depth exists? We set out to explore CH_4 biogeochemical dynamics in two ferruginous lakes to answer these questions. Brownie Lake and Canyon Lake are two meromictic lakes in the Midwest, U.S.A., that have anoxic and Fe-rich bottom waters (>1 mM dissolved Fe below the chemocline; Lambrecht, Wittkop, Katsev, Fakhraee, & Swanner, 2018). Our goal was to evaluate the role of diffusive and non-diffusive CH_4 fluxes to the atmosphere and quantify these CH_4 fluxes in our two ferruginous lakes with different SO_4^{2-} concentrations. More precisely, Canyon Lake with the seawater SO_4^{2-} concentration of ~ 5 μM and Brownie Lake with the seawater SO_4^{2-} of ~ 100 μM can be utilized as analogs to study SO_4^{2-}-driven AOM in the low seawater sulfate of Archean oceans (Crowe et al., 2014; Fakhraee, Crowe, & Katsev, 2018) and the Proterozoic oceans (Fakhraee et al., 2019), respectively. We took direct measurements of the surface CH_4 flux using static flux chambers and measured CH_4 and DIC concentrations and carbon stable isotopes throughout the water column over multiple seasons. We investigated the role of microbes in CH_4 production
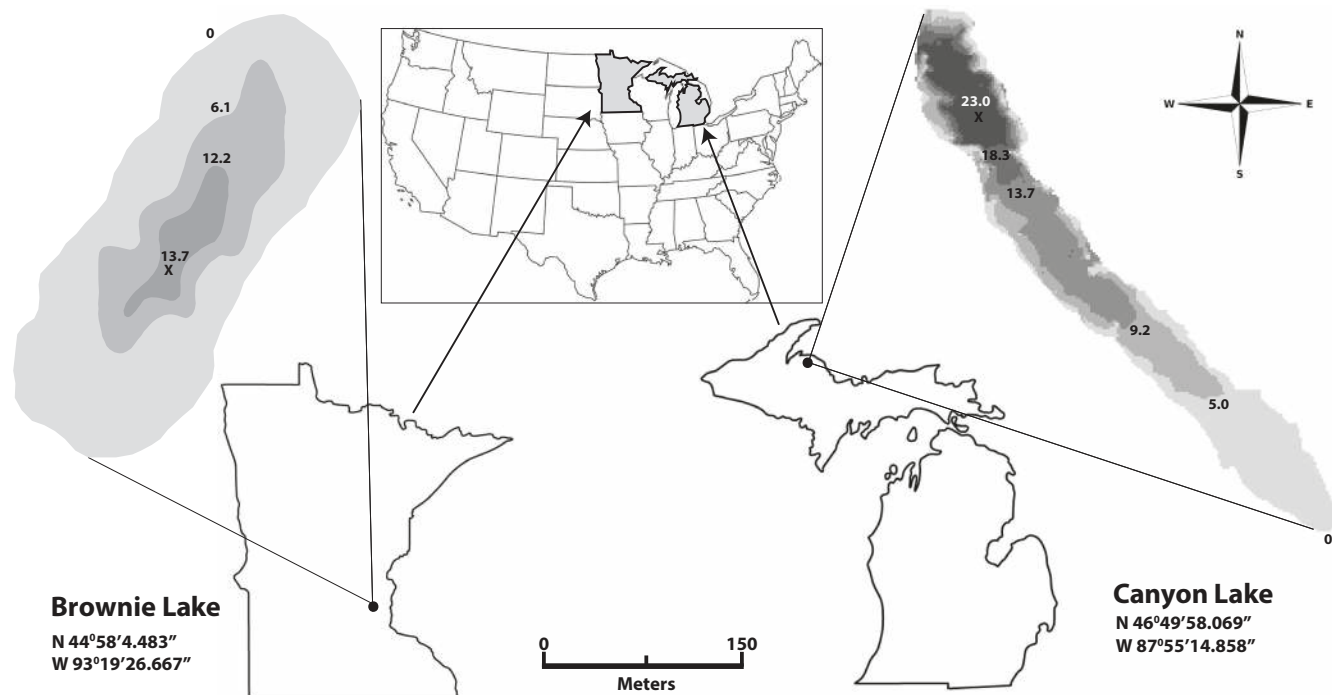
FIGURE 1 Map showing the location of Minnesota and Michigan within the United States (inset), and bathymetric maps of Brownie Lake (Minneapolis, MN) and Canyon Lake (Upper Peninsula of Michigan). The "X" denotes the deepest spot and where samples were obtained

and oxidation through 16S rRNA gene sequencing. Our results were interpreted through reaction-transport modeling to determine the significance of non-diffusional transport pathways for CH_4 emissions from these lakes.

2 | METHODS

2.1 | Site description and sample collection

Brownie Lake is located on the Chain of Lakes in Minneapolis, Minnesota (Myrbo, Murphy, & Stanley, 2011). It is an anthropogenically impacted, eutrophic lake with a surface area of 5 ha and a maximum depth of 14 m, with a relative depth of 5.6%. Brownie Lake became meromictic in the early 1900s due to lake-level lowering, which reduced its surface area and increased its relative depth to favor stratification, and further sheltered it from wind-mixing (Myrbo et al., 2011). The watershed area of Brownie Lake is approximately 150 ha, and the residence time for water within the lake is 2 years (Minneapolis Park and Recreation Board, 2013). Water sources likely include precipitation, groundwater (Goudreault, 1985) and storm sewer runoff (City of Minneapolis GIS Water Quality Model; Barr Engineering, 2019). Road salt, which has been in use since the mid-1900s (Swain, 1984), currently imparts additional stability against mixing (Lambrecht et al., 2018). Furthermore, the thermocline and chemocline are at the same relative location in the water column (~5 m). These profiles, along with water sampling methods, were previously described (Lambrecht et al., 2018). Water samples were collected from the deepest part of Brownie Lake (Figure 1). Sampling campaigns were carried out in May 2017, July 2017, September 2017, and June 2018.

Canyon Lake is a pristine lake nestled in the Huron Mountains in the Upper Peninsula of Michigan. The maximum depth is 23 m, and the approximate surface area is 1 ha (Anderson-Carpenter et al., 2011). Previous seasonal monitoring of Canyon Lake revealed a thermocline near the surface between 3 and 4 m and a persistent chemocline existing at ~17 m (Lambrecht et al., 2018). It is likely naturally meromictic and ferruginous, due to its great depth relative to its small surface area, along with wind protection from the surrounding 20-m-high canyon walls (Lambrecht et al., 2018; Smith, 1940). Water sources to the lake are dominated by precipitation, with nearby seeps and springs supplying some water, and equivocal evidence for a groundwater source (Lambrecht et al., 2018). Canyon Lake was sampled in June 2017, September 2017, and May 2018. Additional details regarding sample collection can be found in Lambrecht et al. (2018).

2.2 | Water column profiles

Dissolved O_2 (LDO model 1 luminescent sensor; detection limit of 3 µM) and chlorophyll *a* were measured by lowering a Hydrolab Series 5 multiprobe (Hach) through the water column of each lake. Sensors were rinsed with deionized water prior to calibration. The dissolved O_2 probe was calibrated using 100% air-saturated water. The chlorophyll *a* sensor has a resolution of ± 0.01 µg/L.

2.3 | Aqueous geochemistry

Samples for dissolved anions (NO_3^-, NO_2^- and SO_4^{2-}; detection limits of 0.1 mg/L) and cations (dissolved Fe and Mn; detection limits of

20 nmol) were filtered using 0.45-μm polyethersulfone (PES) filters (Sartorius). Dissolved cation samples were preserved with HNO_3 at a final concentration of 1%. All samples were kept on ice or at 4°C until analysis. Anions were analyzed using an ion chromatograph (IC) and cations were analyzed by inductively coupled plasma-optical emission spectrometry (ICP-OES) at the University of Minnesota Research Analytical Laboratory.

2.4 | Methane and DIC concentration, isotopes, and flux

Samples for dissolved CH_4 concentrations and isotopes were filtered using 0.45 μm PES filters and directly filled from the sampling line into evacuated Exetainers (Labco, U.K.) with no headspace using a needle attached to the syringe filter. Samples collected in 2018 were additionally preserved with 0.5 ml 6M HCl, with reported concentrations corrected for acid addition. No significant difference in dissolved CH_4 concentration was observed between 2017 and 2018 samples. The field observation of exsolution in waters retrieved from depth was consistent with gas concentrations within the range of CH_4 saturation (e.g., Molofsky et al., 2016) as displayed in our reported values and also consistent with previous reports of a negligible impact of filtering on dissolved CH_4 concentrations (e.g., Alberto et al., 2000). Dissolved inorganic carbon (DIC) concentrations and isotopes were filtered (0.45 μm PES) and injected into exetainers that were He-flushed and contained 1 ml of concentrated phosphoric acid. Methane and DIC concentrations and isotopes were analyzed at the UC-Davis Stable Isotope Facility compared against the Vienna Pee-Dee Belemnite international reference standard, with standard deviations of 0.2 and 0.1 ‰, respectively.

Methane gas fluxes from the lake surface to the atmosphere were measured with static flux chambers using a foam base for flotation. Chamber lids (acrylonitrile) and collars (polyvinyl chloride) had a diameter of 26 cm and a height of 22 cm. Chambers were vented using the design of Xu et al. (2006) to minimize pressure gradients between the chamber and the atmosphere and any wind-induced pressure perturbations due to the Venturi effect. Each flux measurement was calculated using a time series of five gas samples collected every five minutes following closure of the chamber over the collar. Samples were collected by extracting 20 ml of gas through a septum with a needle and gas-tight syringe, which was then injected into an evacuated 12-ml Exetainer vial. Five independent time series were collected per sampling campaign for the open water zone directly above the anoxic sediments. Methane concentrations were measured by gas chromatography at Iowa State University using a flame ionization detector, with a typical coefficient of variation <2% for repeated analyses of standard gases with CH_4 mole fractions between 2 and 10 ppm. Fluxes and standard deviation were calculated from time series of gas concentrations by selecting the optimum model (either a nonlinear diffusion model founded on Fick's law or a linear trend) based on the estimated value of the concentrated least squares criterion fit using the HMR package in R (Pedersen, 2017).

Using this approach, individual chamber flux measurements that exhibited CH_4 spikes consistent with ebullition (Figure S1) were automatically fit to a linear model for parsimony.

2.5 | Flux modeling through the water column at Brownie Lake

Vertical fluxes of CH_4 through the water column by local (diffusional) processes were obtained from a geochemical reaction-transport model using data from May 2017 at Brownie Lake. Transport rates by turbulent eddy diffusion were determined by the balance between the rates of turbulent energy dissipation, which reflects wind forcing, and the strength of the density gradient, characterized by the Brunt–Vaisala stability frequency N (Osborn, 1980). In turbulent epilimnion, the vertical eddy diffusion coefficient (K_Z, m^2/s) often may be phenomenologically approximated (e.g., Katsev et al., 2010) as $K_Z = 3 \times 10^{-10}$ N^{-2}. In the calm, stratified interior the less vigorous energy dissipation is expected to result in lower values of K_Z, with turbulence being slightly higher in the bottom boundary layer (McGinnis & Wuest, 2005). In the absence of physical turbulence measurements, we calculated K_Z in the epilimnion from the measurements-based N and approximated K_Z below the thermocline by fitting the measured chemical profiles, using multiple species to better constrain the model (Figure S2). As this approach necessarily relies on the chemical profiles being approximately steady, seasonal variations and mixing by storms can introduce uncertainty. We therefore restrict the analysis to Brownie Lake, where the range of the oxycline motion is more limited than in Canyon Lake. A one-dimensional reaction-transport model setup in MATLAB simulated vertical profiles of chemical species as steady-state solutions of a boundary-value problem. Decomposition of organic matter was considered throughout the water column at a fixed volume-specific rate R_C (with a fitted value of 0.425 mmol m^{-3} hr^{-1}) and in sediments with the average area-specific flux of F_{sed} (0.416 mmol m^{-2} hr^{-1}). The sediment contribution was apportioned to the corresponding water column depths in accordance with the lake bathymetry. These rates and fluxes were used to calculate the corresponding rates for the consumption of O_2 and the generation of DIC and NH_4^+ (with the C:N ratio of 17). Boundary conditions were prescribed flux for DIC and NH_4^+ at the lake bottom and fixed concentration for O_2 at the lake surface. The $K_Z(z)$ was adjusted as a function of depth to fit all the profiles simultaneously (Figure S2). The turbulent diffusive fluxes of CH_4 through the water column were then calculated from the CH_4 concentration gradient as $F = -K_Z(d[CH_4]/dz)$.

2.6 | Microbiology

Microbial community composition was assessed using high throughput 16S rRNA gene sequencing. A total of 17 depths (13 whole meter and 4 half meter depths) were sampled from Brownie Lake in 2017. Sequencing samples were not collected at every depth in May (2.5,

9, and 13 m excluded) and September (2.5 and 3.5 m excluded). At Canyon Lake, 26 depths (21 whole meter and 5 half meter depths) were sampled in 2017. Samples for sequencing were not collected at 9.5 and 21 m in June and 13.5 and 15.5 m in September.

2.6.1 | Sample collection, filtering, and preservation

Water samples were collected from discrete depths using a 5 L Van Dorn bottle. Individual water samples were subsampled (volumes of ca. 250 ml) and transported in sterilized (10% bleach) high-density polyethylene plastic collection bottles. Samples were stored on ice in a dark cooler (max. two hours) to minimize microbial activity until onshore filtration. A Masterflex portable peristaltic sampler (Cole-Parmer) was used to concentrate cellular biomass of particle-associated microbes, and planktonic microbes (3- and 0.22-μm PES filters; Millipore), respectively. Filters were submerged in a house-made RNA preservation solution (De Wit et al., 2012) in cryovials and stored on dry ice during transport and then a −80°C freezer until DNA extraction.

2.6.2 | DNA extraction, amplicon sequencing, and processing

Extraction of DNA from preserved filters was performed using modified steps from Lever et al. (2015). Filters were thawed and aseptically cut in half. Cellular lysis was performed using a lysis solution (30 mM Tris-hydrochloride, 30 mM EDTA, 800 mM guanidine hydrochloride, 0.5% Triton X-100) at pH 10, followed by a round of freeze-thawing. Nucleic acid extracts were purified using one volume of chloroform-isoamylalcohol (24:1). After purification, DNA was precipitated with one volume of PEG 6000 (30% v/v) and a 0.5 volume of 1.6 M NaCl. Two subsequent washes of the DNA pellet with 70% ethanol were used to remove the PEG-NaCl. DNA pellets were dissolved in PCR grade water.

The V4 region of the 16S rRNA gene was amplified and sequenced with the primer pair 515F (5'-GTGCCAGCMGCCGCGGTAA-3') and 805R (5'-GACTACVSGGGTATCTAAT-3') using a dual index approach (Gohl et al., 2016; Kozich, Westcott, Baxter, Highlander, & Schloss, 2013). Illumina sequencing was performed on the amplicons at the University of Minnesota Genomics Center (Minneapolis, MN) using the MiSeq platform and 2 × 300 bp chemistry. Amplicon reads were processed using Mothur (v1.39) following the standard operating protocol (Schloss et al., 2009). Amplicon pairs were checked for quality, assembled, and aligned to the SILVA v132 database (Pruesse, Peplies, & Glöckner, 2012). Chimeras were checked with Uchime2 (Edgar, 2016), and operational taxonomic units (OTUs) clustered at 97% similarity using the opticlust method (Westcott and Schloss, 2017). Representative OTU sequences were taxonomically classified with the SILVA v132 database using the Naive Bayesian classifier (Wang, Garrity, Tiedje, & Cole, 2007). Graphs were built using the ggplot2 package in R (Wickham, 2016). All amplicon sequences were deposited to the National Center for Biotechnology Information (NCBI) Sequence Read Archive under Project Number PRJNA560450 and Accession numbers SRR9985080-SRR9985286.

3 | RESULTS

3.1 | Geochemical conditions

3.1.1 | Brownie lake

Dissolved O_2 was ~250 μM at 1 m and decreased to undetectable levels by 3–5 m (Figure 2a). The oxycline was located at ~2–3 m in the summer months versus ~4–5 m the spring and fall. The chlorophyll a maximum was consistently located at the base of the oxycline (Figure 2b). Above the oxycline, dissolved Fe concentrations were < 1 μM. Dissolved Fe concentrations increased with depth below the oxycline, reaching > 1 mM at 20 m (Figure 2c). Above the oxycline, dissolved manganese (Mn) was detected (<0.5 μM; Figure 2d). Manganese concentrations peaked below the oxycline, and this trend was observed in all months besides June 2018 where the maximum concentration (~90 μM) was present at the oxycline. Sulfate (SO_4^{2-}) concentrations were highest at or above the oxycline for all months sampled (Figure 2e). The maximum SO_4^{2-} concentration was measured in June 2018 (~85 μM). Below the oxycline, SO_4^{2-} concentrations decreased to < 5 μM near the sediment surface. Nitrate (NO_3^-) was below detection in all months in 2017 (Figure 2f). Nitrate concentrations were maximally ~5 μM below the oxycline in June 2018. Concentrations of nitrite (NO_2^-) were below detection (~2 μM) at all depths measured throughout the 2017–2018 field sampling campaign.

3.1.2 | Canyon lake

Dissolved O_2 was ~250 μM at 1 m and decreased to undetectable levels at 15 m in June and 11 m in September 2017 (Figure 2g). The largest Chl a measurement in 2017 was 3.9 μg/L at 2 m in June 2017 (Figure 2h). The epilimnion contained dissolved Fe between 1 and 2 μM (Figure 2i). Dissolved Fe concentrations began to increase at 15 m and were highest (>1.5 mM) above the sediment–water interface. Dissolved Mn was present in the oxic waters at submicromolar levels (Figure 2j). Dissolved Mn followed a similar trend as Fe down the water column with a maximum concentration of ~140 μM. Sulfate concentrations were ~6 μM in the epilimnion down to 15 m, but then decreased to undetectable levels (Figure 2k). Nitrate reached 8 μM at 12.5 m and 17.5 m in June 2017, but was usually at or just above detection throughout the water column (Figure 2l). Nitrite concentrations were below detection throughout the water column.

3.2 | Methane and DIC

3.2.1 | Brownie lake

In 2017, the highest concentration of CH_4 above the oxycline was 1 μM in May and 9 μM in 2017 (Figure 3a). Methane concentration
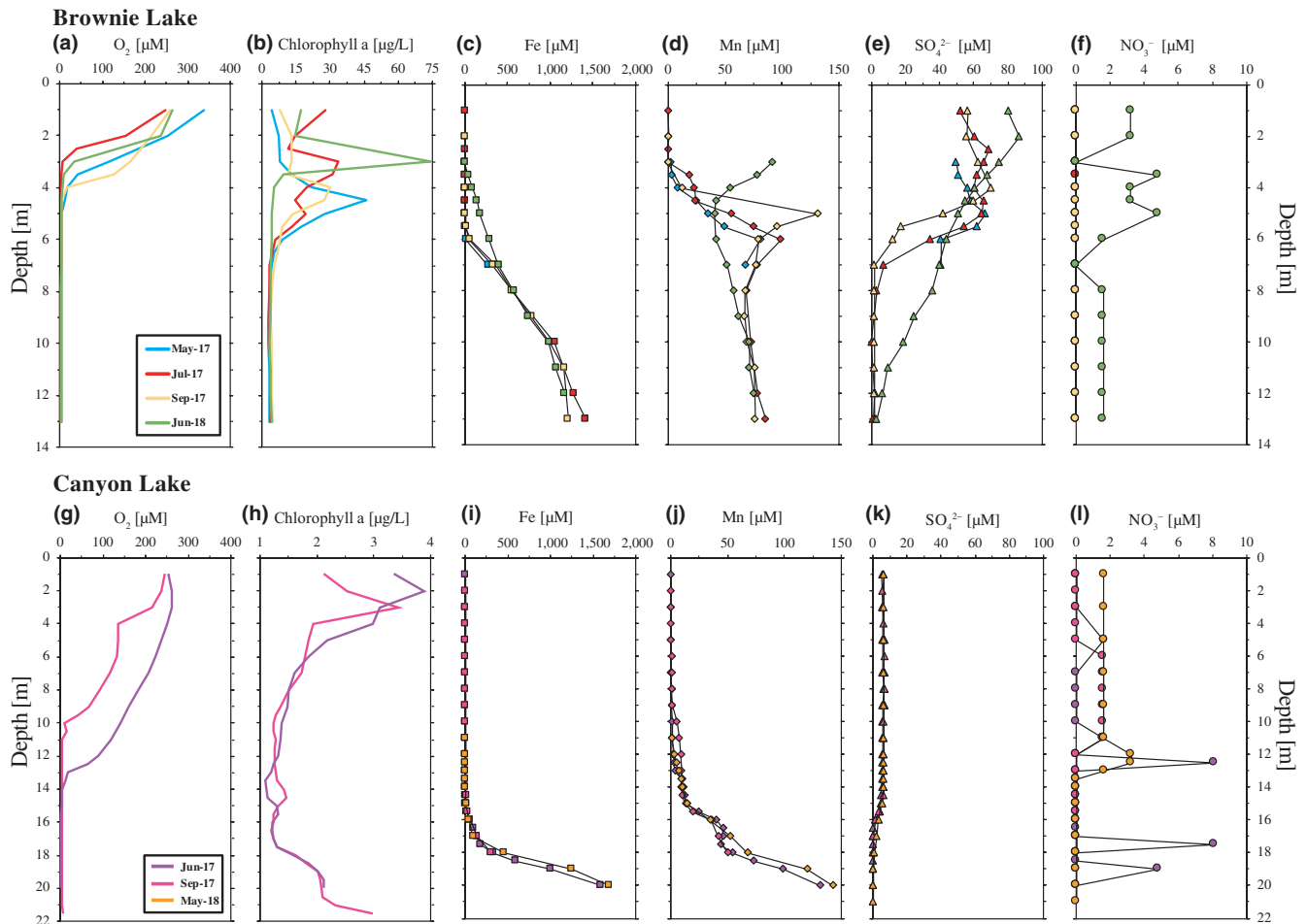
Brownie Lake

Canyon Lake

FIGURE 2 Physicochemical profiles and distribution of dissolved chemical species and ions. (a–f) Brownie Lake. (g–l) Canyon Lake. (a, g) Oxygen (detection limit ~3 µM); (b, h) Chlorophyll *a* profiles. Depth profiles of (c, i) dissolved Fe concentrations quantified by ICP-OES; (d, j) dissolved Mn concentrations determined by ICP-OES; (e, k) sulfate concentrations quantified by IC; and (f, l) nitrate concentrations quantified by IC

was high above the oxycline in June 2018 (~80 µM). Concentrations of CH_4 generally increased steadily with depth below the oxycline. However, the maximum CH_4 concentrations were not measured directly above the sediment–water interface, but rather a meter or two above for all months except July 2017 (Figure 3a). The C-CH_4 isotopic composition ($\delta^{13}C_{CH4}$) was consistently around −64 ‰ below 6 m (Figure 3b). In May, a + 41 ‰ excursion to less negative values occurred between 6 m and 4.5 m. Shifts to less negative values also occurred in September 2017 between 4.5 and 4 m (+16 ‰) and June 2018 between 3.5 and 3 m (+8 ‰) (Figure 3b).

The concentration of dissolved inorganic carbon (DIC) was roughly 1 to 2 mM at 1 m for all months sampled (Figure 3c). DIC concentrations increased deeper into the water column, with similar trends observed between sampling campaigns in 2017. DIC concentrations were higher above 7 m and lower below 7 m in June 2018 compared to sampling campaigns in 2017. The maximum concentration of DIC measured was 14 mM in July (Figure 3c). The $\delta^{13}C_{DIC}$ values were lower deeper through the water column until 5 m in 2017 (Figure 3d). In May and July, $\delta^{13}C_{DIC}$ values exhibited a "sawtooth" pattern around their respective oxyclines, whereby $\delta^{13}C_{DIC}$ values

became lower, then higher, then lower. Below 5 m, the $\delta^{13}C_{DIC}$ values trended toward less negative values (Figure 3d).

3.2.2 | Canyon lake

In the oxic surface waters, CH_4 concentrations varied between 0.1 and 1.5 µM (Figure 3e inset). Methane concentrations increased sharply at 18 m. The reservoir of CH_4 below 18 m was maximally 1.9 mM in May 2018 (Figure 3e). The $\delta^{13}C_{CH4}$ was roughly −72 ‰ below 16 m, except for a small increase to −65 ‰ at 19 m in June 2017 (Figure 3f). Above 16 m, each month varied in their $\delta^{13}C_{CH4}$ profile. In June 2017, the largest excursion occurred between 16 and 13.5 m (+ 72 ‰). Lower $\delta^{13}C_{CH4}$ values were observed higher up in the water column, approaching atmospheric values (~−47 ‰). The $\delta^{13}C_{CH4}$ profile in September 2017 included two excursions toward less negative values between 12 and 11 m (+ 18 ‰) and 5 and 3 m (+ 16 ‰) (Figure 3f). In May 2018, the $\delta^{13}C_{CH4}$ values were consistent throughout the water column (~−72 ‰).

DIC concentrations were highest nearest the sediment–water interface (~6 mM) and decreased toward the surface (Figure 3g). Surface
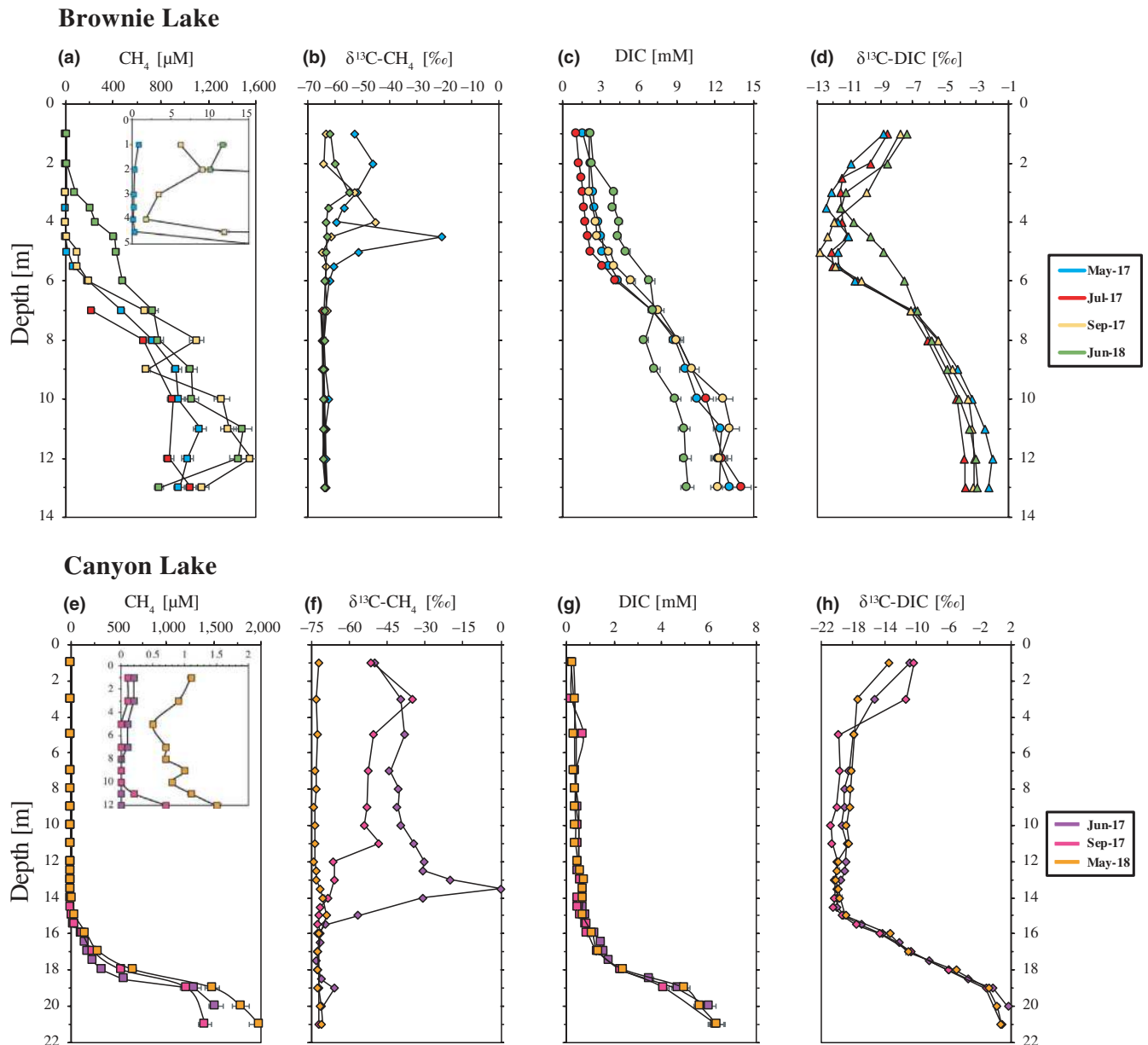
Brownie Lake

Canyon Lake

FIGURE 3 Dissolved methane and DIC profiles. a–d Brownie Lake. e–h Canyon Lake. (a, e) Methane concentration; (b, f) corresponding methane stable carbon isotopes ($\delta^{13}C_{CH4}$); (c, g) DIC concentration; and (d, h) corresponding DIC stable carbon isotopes ($\delta^{13}C_{DIC}$). Methane and DIC concentration measurement error is ± 5%. Isotope standard deviations are less than symbol size

waters had DIC concentrations between 0.2 and 0.3 mM. Above the sediment–water interface $\delta^{13}C_{DIC}$ values were positive, with the highest $\delta^{13}C_{DIC}$ value measured at 20 m in June 2017 (1.64 ‰) (Figure 3h). The $\delta^{13}C_{DIC}$ values trended negative until roughly 14 m (−20 ‰), and remained around this value until 5 m. The surface waters exhibited $\delta^{13}C_{DIC}$ values of ∼−10 ‰ in 2017 and ∼−13 ‰ in 2018.

3.3 | Methane flux

The CH_4 flux at the water–atmosphere interface measured from each sampling campaign, determined by averaging the value of the five independent replicates (Figure S1), is summarized in

Table 1. The standard deviation of each flux measurement is typically larger than the average flux (in general) due to a single large flux relative to other measurements taken during the same sampling campaign (Table S1). The CH_4 flux was highest at Brownie Lake in July 2017 (13.97 mmol m^{-2} hr^{-1}) and at Canyon Lake in May 2018 (0.21 mmol m^{-2} hr^{-1}). At Brownie Lake, there was a positive correlation between CH_4 flux values and chlorophyll a concentrations measured during the same sampling periods (Figure S3). This correlation was not observed at Canyon Lake.

The calibrated vertical transport rates (Figure S2) were used to estimate the turbulent diffusive fluxes of CH_4 within the water column at Brownie Lake in May 2017, but this estimate was not made at Canyon

TABLE 1 Methane flux measurements over open water using static flux chambers

Sampling month	Average CH$_4$ flux (mmol m^{-2} hr^{-1})	Standard deviation	Highest CH$_4$ flux (mmol m^{-2} hr^{-1})	Lowest CH$_4$ flux (mmol m^{-2} hr^{-1})
Brownie lake				
May (2017)	3.48	3.76	10.60	0.19
July (2017)	13.97	14.38	38.83	2.75
September (2017)	1.15	0.45	1.63	0.49
June (2018)	4.23	5.54	13.78	0.34
Canyon lake				
June (2017)	0.04	0.02	0.06	0.02
September (2017)	0.05	0.07	0.17	−0.02*
May (2018)	0.21	0.37	0.92	0.01

Note: *One replicate in September 2017 at Canyon Lake experienced a net consumption of methane instead of a net emission to the atmosphere.
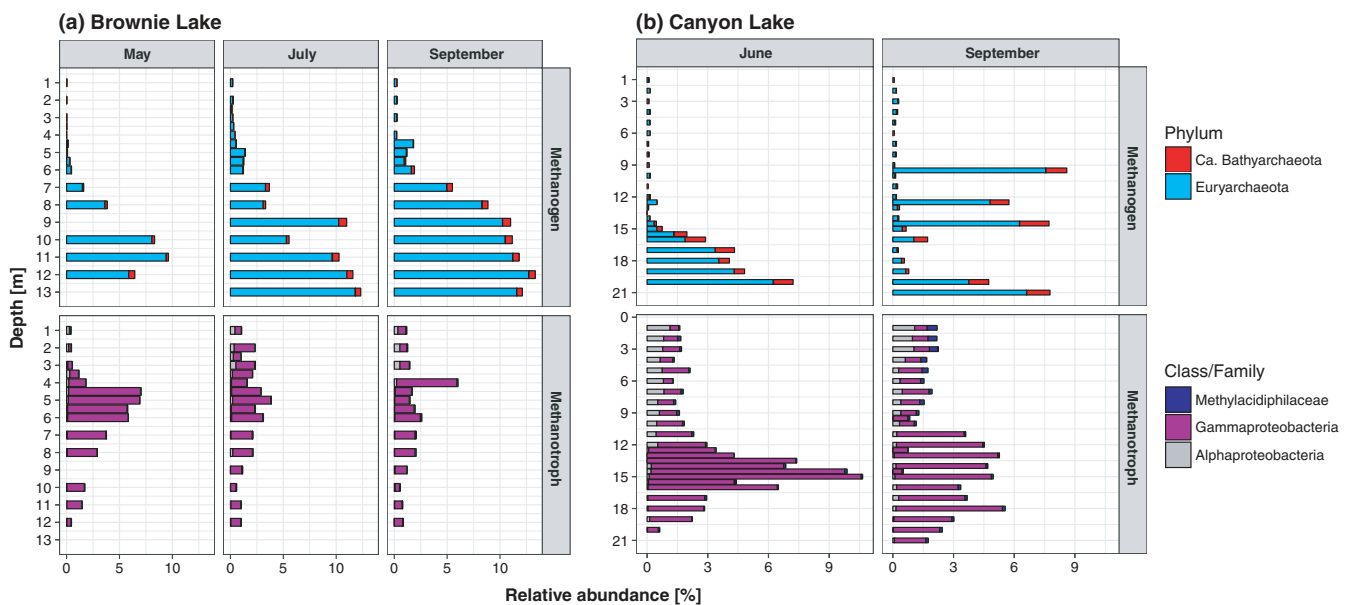

FIGURE 4 Percent relative abundance of methanogens and methanotrophs compared to total sequences recovered at depth from all sampling campaigns in 2017. (a) Brownie Lake. The phylum Euryarchaeota accounted for ~94% of total methanogen sequences. Gammaproteobacteria made up 91% of methanotroph sequences retrieved from the water column. (b) Canyon Lake. Euryarchaeota sequences represented 82% of total methanogens followed by candidate phylum Bathyarchaeota (~ 18%). Gammaproteobacteria were the most abundant methanotrophs at Canyon Lake, totaling 85% of methanotroph sequences

(see Section 2.5). The CH$_4$ concentration gradient in the epilimnion of Brownie Lake was less than 0.07 μM m^{-1}, while the gradient in the thermocline (4.5–5.5 m) was between 30 μM m^{-1} and 100 μM m^{-1}. For the values of K$_z$ in Figure S2, calculations yield turbulent diffusive fluxes in the water column of 0.0025–0.25 mmol m^{-2} hr^{-1} in the epilimnion and 0.05–0.54 mmol m^{-2} hr^{-1} in the thermocline.

3.4 | Microbial composition of methane cycling organisms

Using the Silva taxonomy as a guide, methanogen-associated OTUs and their abundances were filtered from the larger dataset. We

detected five methanogen orders within the Euryarchaeota phylum (*Methanobacteriales, Methanomicrobiales, Methanosarcinales, Methanocellales, and Methanomassiliicoccales*), candidate phylum Bathyarchaeota, and candidate order *Methanofastidiosales* in Brownie Lake and Canyon Lake in 2017 (Figure 4). Euryarchaeota was the most abundant methanogen-containing phylum present in both lakes. *Methanobacteriales* was the most dominant order, encompassing between 64%-75% of methanogen sequences at Brownie Lake and 48%–58% at Canyon Lake in 2017. *Ca. Methanofastidiosales* was the least abundant methanogen present at both lakes (Brownie: 16 total sequences recovered; Canyon: 6 total sequences recovered). No sequences were identified from the novel candidate phylum

Verstraetearchaeota. To ensure the remaining archaeal sequences were indeed methanogens and not ANME archaea, all candidate methanogenic OTU sequences were compared to a database of ANME sequences identified from a low SO_4^{2-}, Fe-rich freshwater sediment using BLAST (Boratyn et al., 2013; Weber, Habicht, & Thamdrup, 2017). Based on BLAST similarity, we identified no ANME-like sequences (<90% similarity) within our dataset similar to these putative ANME reference sequences. A BLAST approach was chosen due to the gaps in the archaeal taxonomy; *for example*, many of the sequences were labeled as uncultured or unknown beyond the family or genus level.

Type 1 methanotrophs (within the Gammaproteobacteria) were the most abundant aerobic MOB retrieved from both water columns, followed by Type 2 methanotrophs (within the Alphaproteobacteria) in 2017 (Figure 4). Type 2 methanotrophs were more abundant in Canyon Lake than in Brownie Lake above the oxycline. The family *Methylacidiphilaceae* has recently been described as aerobic MOB that grow in acidic geothermal areas (Op den Camp, Islam, & Stott, 2009 and references therein). However, *Methylacidiphilaceae*-like OTUs were present throughout the circumneutral water columns of Brownie Lake and Canyon Lake in 2017. Thirteen sequences (0.003% of total sequences recovered) from a member belonging to phylum Rokubacteria (formerly NC10) known to perform nitrite-dependent anaerobic oxidation of CH_4, genus *Ca.* Methylomirabilis, were recovered in 2017 from Brownie Lake despite NO_2^- levels below our detection. Similarly, six *Ca.* Methylomirabilis sequences (0.001% of total sequences recovered) were retrieved from Canyon Lake in 2017.

4 | DISCUSSION

4.1 | Methane flux modeling conflicts with direct measurements

A clear result of the comparison of atmospheric CH_4 fluxes directly measured by static flux chambers versus calculated diffusive fluxes based on the concentration profiles of CH_4 is that measured values are 1000–10,000× higher than calculated values, for Canyon and Brownie, respectively. It is also clear that modeling of the turbulent diffusive flux through the water column of Brownie Lake (Figure S2) indicates a significant non-zero flux of CH_4, despite ecological and geochemical evidence for vigorous aerobic CH_4 oxidation. Therefore, other pathways for CH_4 transport from the lake to atmosphere must be invoked. As our flux measurements come from the middle of the lakes, a plant-mediated flux can be excluded. In addition, both lakes are meromictic, which precludes a storage flux released by seasonal lake turnover (Bastviken, Cole, Pace, & Tranvik, 2004). The other pathway for gas to escape is ebullition, a transport mechanism with high spatiotemporal variability (Bastviken et al., 2004). Ebullition is frequently observed to be dominant in lakes, but is rarely quantified with regard to CH_4 emissions (Sanches, Guenet, Marinho, Barros, & Assis Esteves, 2019). It is especially important in shallow lakes (<20 m deep) as bubbles have lower hydrostatic

pressure to overcome (Bastviken et al., 2004; Bastviken, Tranvik, Downing, Crill, & Enrich-Prast, 2011). Modeling of deeper ferruginous lakes, such as Lake Matano, Kabuno Bay, and Lake Pavin, suggests that atmospheric CH_4 fluxes should be small because the slow transport of CH_4 by turbulent diffusion allows for oxidation in the water columns before CH_4 reaches the atmosphere (Borges et al., 2011; Crowe et al., 2011; Lopes et al., 2011). Similar modeling in relatively shallow Lake La Cruz assumes that CH_4 is transported upwards in the lake via diffusion and is likely completely oxidized by microbes in the water column (Oswald, Jegge, et al., 2016a). However, without direct measurements, the contribution of ebullition to the total CH_4 flux is not considered. For example, other authors have noted rising bubbles that contain roughly 50% CH_4 reaching the atmosphere in Lake La Cruz (Camacho, Miracle, Romero-Viana, Picazo, & Vicente, 2017).

Increased sedimentary gas venting episodes have been observed to occur with precipitous drops in hydrostatic pressure due to changes of water level in lakes and reservoirs (Casper, Maberly, Hall, & Finlay, 2000; Chanton, Martens, & Kelley, 1989; Scandella et al., 2016). In 1916, a canal was created to connect Brownie Lake to nearby Cedar Lake, which reduced the water level 3 m over the course of a few days (Swain, 1984; Wirth, 1946). Mechanistically, decreasing hydrostatic pressure reduces stress causing gas pockets to become more ductile in sediments, and when stress reaches a critical point, these gas pockets create vertical channels out of the sediments (Boudreau et al., 2005; Jain & Juanes, 2009). The precipitous water level drop that Brownie Lake experienced would have caused rapid degassing in the sediments, creating conduits for future bubble transport out of the sediment. Once a conduit has formed in sediment, subsequent bubbles can re-open the fracture easily (Algar, Boudreau, & Barry, 2011; Scandella, Delwiche, Hemond, & Juanes, 2017). We suggest that these conduits give rise to the high non-diffusive fluxes from Brownie Lake, likely through ebullition.

Another factor contributing to the CH_4 cycle in Brownie Lake is CH_4 production. Eutrophic lakes have higher abundances of photosynthetic microbes and higher rates of primary production (Schindler, 1978). NPP has been shown to have a linear relationship with CH_4 flux across diverse lakes (Davidson et al., 2015; Huttunen et al., 2003; Juutinen et al., 2009) and wetlands (Whiting & Chanton, 1993). Therefore, net primary productivity (NPP) could represent a crucial control on CH_4 emissions from Brownie Lake. This is especially apparent in May 2017 where cyanobacteria were ~10% of the total microbial 16S rRNA gene sequences recovered in the photic zone. DelSontro, Boutet, St-Pierre, Giorgio, and Prairie (2016) noted a positive, significant correlation between Chl *a* concentration (0.2 m below the water column surface) and CH_4 fluxes (both diffusive and ebullitive) from their pond and lake field sites. This further suggests that more productive systems tend to have higher fluxes. This relationship is indicated at Brownie Lake from the correlation of Chl *a* present in the surface waters (1 m) and the measured flux of CH_4 during the concurrent sampling campaigns ($R^2 = 0.79$; Figure S3). Such a relationship was not observed at Canyon Lake. There, the increase in Chl *a* below the chemocline (~17 m) is most likely

representative of a > 4× increase in dissolved organic carbon (DOC) concentrations from 17 m to 21 m across the chemocline (data not shown). Organics in the water column have the potential to enhance light scatter and increase readings on the Chl a sensor (Hach; https://www.ott.com/download/fluorescence-white-paper/). The Chl a concentration below the chemocline corresponds with the increase of DOC concentration and is therefore an artifact of the matrix of the water column at these depths.

Unlike Brownie Lake, one-dimensional modeling to estimate turbulent diffusion of CH_4 within the water column is not appropriate at Canyon Lake where the vertical chemical profiles (e.g O_2) above the monimolimnion fluctuate dramatically through the seasons. Canyon Lake CH_4 concentration profiles display a distinctive trend where concentration is below detection (or less than one micromolar) in the oxic water and then increases toward the surface (Figure 3e inset). As diffusion cannot occur against the concentration gradient, the CH_4 in the surface layer most likely originates from lateral transport of CH_4 produced in littoral sediments (Table S2). Another source of CH_4 in the oxic waters could be aerobic demethylation of methylphosphonate (e.g., Wang, Dore, & McDermott, 2017; Yao, Henny, & Maresca, 2016); however, this was not assessed in this study.

4.2 | Ferruginous conditions favor methanogenesis

We have shown evidence supporting active methanogenesis in Brownie Lake, possibly in both the sediments and water column. We also observed both Fe(II)- and Fe(III)-bearing mineral phases in Brownie Lake sediment cores (Figure S4), indicating that while Fe(III) is available for Fe(III) reduction in the sediments, it is persisting despite very reducing conditions. The overwhelming majority of recovered methanogen sequence reads in both water columns belong to hydrogenotrophic organisms as opposed to acetoclastic organisms, yet the C- and H-isotopic composition of CH_4 implies a mixture of the two (Table S3). Hydrogenotrophic methanogenesis under ferruginous conditions is consistent with prior studies (see Bray et al., 2017). The persistence of Fe(III) oxides to sediment has also been observed in other seasonally stratified ferruginous lakes (Davison, 1993). Crowe et al. (2011) suggested that Fe(III)-bearing minerals may be resistant to microbial reduction in ferruginous systems, and our data support this. A precedent for the dominant role of methanogenesis in organic carbon degradation has also been put forward by the activity measurements of different anaerobic pathways in ferruginous Lake Matano and Lake Svetloe (Crowe et al., 2011; Savvichev et al., 2017), and similar work would be useful in Brownie and Canyon Lakes.

Brownie Lake and Canyon Lake harbor higher CH_4 concentrations when compared to lakes that experience turnover with similar depths in the Midwestern United States. During our sampling interval, the maximum CH_4 concentration in the anoxic monimolimnion at Canyon Lake was 1.9 mM in May 2018 (Figure 3e). Brownie Lake CH_4 concentrations were not quite as high, reaching 1.5 mM in September 2017 (Figure 3a). In contrast, Asylum Lake in Michigan (max. depth 15.8 m) is a monomictic lake and CH_4 accumulates to 612 μM maximally in the anoxic hypolimnia (Dupuis et al., 2019). North Lake (max. depth 20 m), also in Michigan, is a dimictic lake that accumulates less CH_4 in its anoxic hypolimnia (183 μM) (Dupuis et al., 2019). Salient to the discussion is that the months with the highest CH_4 accumulation in Asylum and North Lakes documented by Dupuis et al. (2019) were also the same months which documented the highest Fe(II) concentrations (Asylum, 4 μM; North, 49 μM). The high accumulation of CH_4 in the ferruginous meromictic water columns of Brownie and Canyon Lakes compared to lakes that turnover with orders of magnitude less Fe demonstrates the importance of understanding the interaction of the Fe and CH_4 cycles in these lacustrine systems.

4.3 | Water column methanogenesis

Methanogenesis conventionally occurs in lacustrine sediments where fermentation of organic matter provides the organic and inorganic compounds necessary for methanogenesis in high concentrations relative to the water column (Rudd & Hamilton, 1978). However, 16S rRNA gene amplicon sequencing in Brownie Lake from 2017 revealed that ~31% of sequences at 11 and 12 m belonged to known methanogen orders (Figure 4a). In addition, CH_4 concentrations at 11 and 12 m were elevated compared to CH_4 concentrations nearest the sediment (Figure 3a). The $\delta^{13}C_{CH4}$ signatures at 11 and 12 m (−64‰; Figure 3b) are well within the range of −50 to −110 ‰, which is consistent with biogenic CH_4 production (Table S3; Whiticar, 1999). This anomaly contrasts with the geochemical reaction-transport modeling that predicted that reduced species would be at their highest concentrations at the sediment–water interface (Figure S2) and implicates active water column methanogenesis in the monimolimnion of Brownie Lake. While relative abundance of organisms does not necessarily correspond to biogeochemical activity, these observations provide circumstantial evidence for further studies to investigate the relationship between methanogens and pelagic CH_4 production. Furthermore, water column methanogenesis has been noted at Lake Matano (Crowe et al., 2011) and Lake Svetloe, although rates were two orders of magnitude less than rates measured in the sediment (Savvichev et al., 2017).

The differences between the Mn profiles is likely driven by differences in the magnitude of sulfur cycling between sites (greater in Brownie Lake, less significant in Canyon Lake), as well as the nature of the oxycline (compressed in Brownie Lake, elongated in Canyon Lake). The combination of enhanced sulfur cycling and close proximity to oxic waters in Brownie Lake accentuates the concentrations of Mn in the oxycline (e.g., Herndon, Havig, Singer, McCormick, & Kump, 2018; Jones et al., 2011). Interestingly, Canyon Lake displays a similar magnitude of overall dissolved Mn enrichment relative to Brownie Lake, but the location of the enrichment varies. At Canyon Lake, the strongest Mn enrichment is located just above the sediment–water interface (Figure 2j). In contrast, the zone of dissolved Mn enrichment at Brownie Lake migrates seasonally, with peak enrichment shifting up to and just above the chemocline in summer/

early fall (Figure 2d), but reverting to a Canyon-like pattern with the highest concentration near the sediment–water interface in winter. Consistent with their contrasting behaviors in suboxic environments, dissolved Mn migrates higher into the water column than dissolved Fe in Canyon Lake, but the Mn profile is subdued relative to Brownie. This can be explained by the infrequent O_2 penetration to the deep waters of Canyon and is perhaps reflective of the pattern of Mn enrichment implied in Archean settings where O_2 accumulation was limited to spatially restricted oases (e.g., Planavsky et al., 2011).

4.4 | Methanotrophy within the water column

There is a general decrease in CH_4 concentration from the sediment–water interface toward the oxycline, signifying diffusional transport of CH_4 out of sediments, except for peaks in the concentration at 11 and 12 m in Brownie Lake. Methane oxidation, as evident by the less negative $\delta^{13}C_{CH4}$ values above 6 m, occurs at or immediately below the chemocline (Figure 3b). A $\delta^{13}C_{CH4}$ pattern consistent with methanotrophy created excursions toward less negative $\delta^{13}C_{CH4}$ values at 4.5 m in May 2017 (−51 ‰ to −21 ‰), 4 m in September 2017 (−62 ‰ to −45 ‰), and 3 m in June 2018 (−63 ‰ to −55 ‰). Furthermore, the "sawtooth" pattern of the $\delta^{13}C_{DIC}$ values at the chemocline, most notably observed at Brownie Lake in May and July 2017, is indicative of the oxidation of isotopically light CH_4 to DIC (Figure 3d). Low (but detectable) O_2 concentrations, a peak in the relative abundance of aerobic MOB, and a consistent shift to higher $\delta^{13}C_{CH4}$ isotopes indicate a role for aerobic MOB in CH_4 oxidation at the oxycline. Canyon Lake displays similar trends in CH_4, $\delta^{13}C_{CH4}$, and aerobic MOB in June 2017. Notable in June 2017 was an extreme + 72 ‰ shift between 16 and 13.5 m. Similar observations in the $\delta^{13}C_{CH4}$ isotope profiles have been attributed to aerobic MOB at the oxic–anoxic boundary in other lakes (e.g., Blees et al., 2014; Oswald, Jegge, et al., 2016a; Schubert et al., 2006).

Our microbial composition analysis points to the significant role of aerobic MOB in CH_4 removal; however, oxidation of biologically produced CH_4 using other electron acceptors (SO_4^{2-}, NO_3^-, Fe- and Mn-hydroxides) is a possibility. Specifically, while SO_4^{2-}-driven anaerobic oxidation of methane (S-AOM) has largely been viewed to be insubstantial under low SO_4^{2-} conditions, recent studies have shown that S-AOM can, in fact, provide an efficient barrier to CH_4 emission from lake sediment even at SO_4^{2-} concentrations < 200 μM/L (Norði, Thamdrup, & Schubert, 2013; Weber, Thamdrup, & Habicht, 2016). Moreover, in incubation experiments, oxidation of CH_4 in the water column of Lake Kivu, a deep meromictic tropical lake, was diminished when SO_4^{2-}-reducing organisms were inhibited (Roland et al., 2018).

We present supporting thermodynamic calculations, specifically the Gibbs free energy for the S-AOM pathway under a range of CH_4 and SO_4^{2-} concentrations encompassing those found in Brownie and Canyon Lakes (Figure S5). Our results show that S-AOM in both lakes may not provide adequate energy for biomass production, implying S-AOM is likely unimportant in CH_4 cycling. Generally, the ultimate thermodynamic constraint on metabolic

reactions is the need to use the energy provided by the reaction in adenosine triphosphate (ATP) formation. More precisely, the energy produced by a chemical reaction is used to translocate protons within the cell membrane, which then utilize a proton motive force to synthesize ATP. The minimum energy threshold needed for ATP production under normal cellular conditions is ~50 kJ/mol. As there is always an inefficiency involved with the ATP production process, the realistic minimum value is likely around 60 kJ/mol (Schink, 2002). Three protons are normally required to generate an ATP molecule, though some organisms translocate four or more (Stock, Leslie, & Walker, 1999; Taupp, Constan, & Hallam, 2010; Van Walraven, Strotmann, Schwarz, & Rumberg, 1996). In the case of a four-proton translocation system where each proton provides energy for ATP synthesis, the minimum energy required to oxidize one mole of CH_4 is 15 kJ (Taupp et al., 2010). Note that within a syntrophic consortium, such as the ANME and SO_4^{2-}-reducing bacteria, the energy derived from substrate oxidization is shared between the two species and therefore must yield at least 30 kJ/mol. It is also suggested that since there is only a small amount of energy available by AOM, and only one partner in a two partner syntrophy should be able to derive energy from this reaction to produce ATP, CH_4 oxidation coupled to SO_4^{2-} reduction is a co-metabolic activity that may not involve direct electron transfer (Schink, 1997). Using the assumption that a minimum of 30 kJ/mol of energy is needed to perform AOM, and comparing this minimum value to our thermodynamic estimates in Brownie and Canyon Lakes, our results show just a narrow range of conditions under which S-AOM can pass the minimum limit and produce enough energy for ATP production (Figure S5).

The observed range of SO_4^{2-} and CH_4 concentrations in Canyon Lake points to a very small, if any, possibility for S-AOM in the water column. On the other hand, the chemocline of Brownie Lake harbors a combination of 10s of μM of SO_4^{2-} and 100s μM of CH_4, which can potentially pass the minimum threshold for ATP production and bioenergetically justify the presence of S-AOM in the lake. Overall, our thermodynamic calculations, along with the microbial composition analysis, seem not to support a great importance of S-AOM in the cycling of CH_4. Placed in the context of early Earth ocean chemistry, our results from Canyon Lake suggest that in the anoxic Archean oceans where seawater SO_4^{2-} was low (<10 μM; Crowe et al., 2014), the S-AOM would likely have played a minor role in CH_4 removal. This, in turn, would allow biologically produced CH_4 to escape from the ocean via diffusion through an anoxic surface ocean and support greenhouse warming during the Archean. In addition, it is important to note that the salinity of the Archean ocean is hypothesized to have been 1.5–2× the modern value (35 ‰; Knauth, 2005), and the maximum salinity values of Brownie Lake and Canyon Lake are 10–100× less than the modern ocean (Figure S6). The correlation (or possible lack thereof) between salinity and the microbial community and CH_4 production and oxidation was not assessed during this study, but has been addressed by other authors in similar lakes (e.g., Dupuis et al., 2019).

4.5 | Methane emissions from ancient ferruginous oceans

The microbiological processes and biogeochemical cycling occurring in ferruginous meromictic lakes are often invoked as having analogy to redox-stratified, ferruginous oceans of the Archean and Proterozoic eons (Poulton & Canfield, 2011). For instance, processes of microbial Fe(II) oxidation and Fe(III) reduction have been observed to impact the carbon cycle across the O_2 and Fe(II) redoxcline in lakes (e.g., Berg et al., 2019; Berg et al., 2016; Camacho, Walter, et al., 2017; Gorlenko, Vainstein, & Chebotarev, 1980; Savvichev et al., 2017; Walter et al., 2014). These processes are also envisioned to have impacted the carbon cycle in ferruginous oceans (Posth, Konhauser, & Kappler, 2013). Recent work in these lakes has highlighted the utility of such lakes to investigate microbiological and geochemical aspects of CH_4 cycling (e.g., Crowe et al., 2011; Dupuis et al., 2019; Lopes et al., 2011; Oswald, Jegge, et al., 2016a; Savvichev et al., 2017). The CH_4 cycle in ferruginous lakes has been most thoroughly discussed in the context of Indonesian Lake Matano and has given rise to active debate surrounding organic matter preservation in ferruginous oceans (Crowe et al., 2011; Kuntz, Laakso, Schrag, & Crowe, 2015; Laakso & Schrag, 2019). Nonetheless, the global climate system of the Archean appears sensitive to the specific microbial pathways involved in CH_4 and carbon cycling in ferruginous oceans (Ozaki, Tajika, Hong, Nakagawa, & Reinhard, 2018). The observation that microbial communities can strongly influence their environment highlights the importance of identifying the effects a ferruginous water column has on methanogenesis and CH_4 fluxes, which can be investigated in modern lakes (Laakso and Schrag, 2018).

The range of CH_4 fluxes from ferruginous, meromictic lakes is reported in Table S4. While the flux values reported here for Brownie and Canyon Lakes represent direct measurements that incorporate fluxes from multiple emission pathways, the values reported for Kabuno Bay, Lake Pavin, Lake La Cruz, and Lake Matano were calculated from water column concentration profiles and hence only provide information on the flux by turbulent diffusion. As we discuss here, CH_4 emission from ferruginous lakes reflects a complex set of physical, chemical, and biological processes. Our data indicate ebullition from relatively shallow sediments is likely for Brownie Lake, and lateral transport of CH_4 from littoral sediments in Canyon Lake. Importantly, these physical transport processes may give rise to significant non-diffusive fluxes, which, in addition to diffusional fluxes, may change CH_4 flux estimates considerably.

The microbial production of greenhouse gases under ferruginous conditions has led to the suggestion that gases such as CH_4 or N_2O could have been important in regulating early Earth's climate when solar luminosities were lower (e.g., Kasting, 2005; Stanton et al., 2018). However, biosphere models for oceanic CH_4 emissions during the Archean and Proterozoic eons generally only consider transport of CH_4 by turbulent diffusion (Olson, Reinhard, & Lyons, 2016), which favors efficient oxidation of CH_4 at an oxycline (Oswald, Jegge, et al., 2016a). Ebullition and other non-diffusive gas transport processes are omitted, despite the

acknowledgement of the importance of such pathways in transport of CH_4 from near-shore environments (e.g., Daines & Lenton, 2016). Pelagic fluxes of CH_4 from the Archean/Paleoproterozoic ocean were likely small due to low productivity and deep water columns, but the relatively shallow waters on continental margins are hypothesized to have been more productive and have higher inputs of labile organic carbon (e.g. Laakso and Schrag, 2014). Furthermore, organic carbon mineralization is slower and preservation higher under anoxic conditions (Katsev & Crowe, 2015), which were widespread. For comparison, the flux of CH_4 from the modern ocean is in the range of 11–18 Tg CH_4 per year, and 75% of this total is attributed to coastal areas (Bange et al., 1994), likely linked to intense primary productivity (Borges, Champenois, Gypens, Delille, & Harlay, 2016).

In addition to diffusional transport of CH_4, the unique physical transport mechanisms in marine systems need to be considered, as they can differ quite substantially from lakes. In very shallow sediments (i.e., 8 m), CH_4 can be released through ebullition (Algar et al., 2011). Methane seeps as deep as 30 m have also been recognized as having a significant CH_4 flux to the atmosphere, which may be related to ebullition of bubbles in well-mixed waters (Borges et al., 2016). While not a significant source of CH_4 to the atmosphere today, upwelling (i.e., advection) can transport CH_4 from deep oceans (e.g., Kock, Gebhardt, & Bange, 2008). Another mechanism of CH_4 release to the atmosphere is natural gas seepage on the continental shelf. Although these gas seepages are rare, they can significantly contribute to total modern marine CH_4 emissions. For example, gas seepages from the continental shelf of the United Kingdom account for up to 40% of total CH_4 emissions in that area (Judd et al., 1997). In addition, sea-level fluctuations due to glaciation–deglaciation can cause release of CH_4 due to changes in hydrostatic pressure, currents, and bottom water temperatures (Portilho-Ramos et al., 2018). Finally, CH_4 hydrates found in continental margin sediments could also be destabilized by earthquakes (Mienert, Posewang, & Baumann, 1998) and turbidity currents (Shakhova et al., 2014). These observations highlight the importance of considering all possible emission pathways for CH_4 when modeling past marine CH_4 fluxes.

Our findings of non-diffusive fluxes of CH_4 to the atmosphere from meromictic ferruginous lakes with active CH_4 cycles demonstrate how non-diffusive transport mechanisms can create large CH_4 fluxes. While lakes and oceans have very different physical transport mechanisms for dissolved gases, our work highlights that all relevant transport processes, and direct measurements, need to be considered for either type of system. In support of this assertion, CH_4 production in shallow continental margins where non-diffusive transport of CH_4 to the atmosphere would be possible (<100 m; McGinnis et al., 2006) may have produced a considerable amount of CH_4 from at least 3.5 Ga until these environments became oxic at ~ 2.7 Ga (Fakhraee et al., 2018). Quantifying non-diffusive transport of CH_4 and incorporating these values into atmospheric models may strengthen the argument that atmospheric CH_4 helped to modulate temperature during the mid to late Archean in the presence of a less luminous Sun (i.e., Faint Young Sun Paradox).

ORCID

Nicholas Lambrecht 🔟 https://orcid.org/0000-0003-4993-6662

REFERENCES

Alberto, M. C. R., Arah, J. R. M., Neue, H. U., Wassmann, R., Lantin, R. S., Aduna, J. B., & Bronson, K. F. (2000). A sampling technique for the determination of dissolved methane in soil solution. *Chemosphere - Global Change Science*, *2*(1), 57–63. https://doi.org/10.1016/S1465-9972(99)00044-6

Algar, C. K., Boudreau, B. P., & Barry, M. A. (2011). Release of multiple bubbles from cohesive sediments. *Geophysical Research Letters*, *38*. https://doi.org/10.1029/2011GL046870

Anderson-Carpenter, L. L., McLachlan, J. S., Jackson, S. T., Kuch, M., Lumibao, C. Y., & Poinar, H. N. (2011). Ancient DNA from lake sediments: Bridging the gap between paleoecology and genetics. *BMC Evolutionary Biology*, *11*. https://doi.org/10.1186/1471-2148-11-30

Aselmann, I., & Crutzen, P. J. (1989). Global distribution of natural freshwater wetlands and rice paddies, their net primary productivity, seasonality and possible methane emissions. *Journal of Atmospheric Chemistry*, *8*(4), 307–358. https://doi.org/10.1007/BF00052709

Bastviken, D., Cole, J., Pace, M., & Tranvik, L. (2004). Methane emissions from lakes: Dependence of lake characteristics, two regional assessments, and a global estimate. *Global Biogeochemical Cycles*, *18*. https://doi.org/10.1029/2004GB002238

Bastviken, D., Tranvik, L. J., Downing, J. A., Crill, P. M., & Enrich-Prast, A. (2011). Freshwater methane emissions offset the continental carbon sink. *Science*, *331*, 50. https://doi.org/10.1126/science.1196808

Berg, J. S., Jézéquel, D., Duverger, A., Lamy, D., Laberty-Robert, C., & Miot, J. (2019). Microbial diversity involved in iron and cryptic sulfur cycling in the ferruginous, low-sulfate waters of Lake Pavin. *PLoS ONE*, *14*(2), e0212787.

Berg, J. S., Michellod, D., Pjevac, P., Martinez-Perez, C., Buckner, C. R., Hach, P. F.,...Kuypers, M. M.M. (2016). Intensive cryptic microbial iron cycling in the low iron water column of the meromictic Lake Cadagno. *Environmental Microbiology*, *18*(12), 5288–5302.

Biderre-Petit, C., Jézéquel, D., Dugat-Bony, E., Lopes, F., Kuever, J., Borrel, G., ... Peyret, P. (2011). Identification of microbial communities involved in the methane cycle of a freshwater meromictic lake. *FEMS Microbiology Ecology*, *77*, 533–545. https://doi.org/10.1111/j.1574-6941.2011.01134.x

Blees, J., Niemann, H., Wenk, C. B., Zopfi, J., Schubert, C. J., Kirf, M. K., ... Lehmann, M. F. (2014). Micro-aerobic bacterial methane oxidation in the chemocline and anoxic water column of deep south-Alpine Lake Lugano (Switzerland). *Limnology and Oceanography*, *59*, 311–324. https://doi.org/10.4319/lo.2014.59.2.0311

Boratyn, G. M., Camacho, C., Cooper, P. S., Coulouris, G., Fong, A., Ma, N., et al. (2013). BLAST: a more efficient report with usability improvements. *Nucleic acids research*, *41*(W1), W29–W33.

Borges, A. V., Abril, G., Delille, B., Descy, J. P., & Darchambeau, F. (2011). Diffusive methane emissions to the atmosphere from Lake Kivu (Eastern Africa). *Journal of Geophysical Research*, *116*. https://doi.org/10.1029/2011JG001673

Borges, A. V., Champenois, W., Gypens, N., Delille, B., & Harlay, J. (2016). Massive marine methane emissions from near-shore shallow coastal areas. *Scientific Reports*, *6*, 27908.

Boudreau, B. P., Algar, C., Johnson, B. D., Croudace, I., Reed, A., Furukawa, Y., ... Gardiner, B. S. (2005). Bubble growth and rise in soft sediments. *Geology*, *33*, 517–520. https://doi.org/10.1130/G21259.1

Bray, M. S., Wu, J., Reed, B. C., Kretz, C. B., Belli, K. M., Simister, R. L., ... Glass, J. B. (2017). Shifting microbial communities sustain multiyear iron reduction and methanogenesis in ferruginous sediment incubations. *Geobiology*, *15*(5), 678–689. https://doi.org/10.1111/gbi.12239

Camacho, A., Miracle, M. R., Romero-Viana, L., Picazo, A., & Vicente, E. (2017). Lake La Cruz, an Iron-Rich Karstic Meromictic Lake in Central Spain. In R. D., Gulati, A. G., Degermendzhi & E. S., Zadereev (Eds.), *Ecology of meromictic lakes* (pp. 187–233). Cham, Switzerland: Springer.

Camacho, A., Walter, X. A., Picazo, A., & Zopfi, J. (2017). Photoferrotrophy: Remains of an ancient photosynthesis in modern environments. *Frontiers in Microbiology*, *8*, 323.

Canfield, D. E. (2005). The early history of atmospheric oxygen: homage to Robert M. Garrels. *Annual Review of Earth and Planetary Sciences*, *33*(1), 1–36. https://doi.org/10.1146/annurev.earth.33.092203.122711

Canfield, D. E., Poulton, S. W., & Narbonne, G. M. (2007). Late-Neoproterozoic deep-ocean oxygenation and the rise of animal life. *Science*, *315*(5808), 92–95. https://doi.org/10.1126/science.1135013

Casper, P., Maberly, S. C., Hall, G. H., & Finlay, B. J. (2000). Fluxes of methane and carbon dioxide from a small productive lake to the atmosphere. *Biogeochemistry*, *49*, 1–19. https://doi.org/10.1023/A:1006269900174

Catling, D. C., Claire, M. W., & Zahnle, K. J. (2007). Anaerobic methanotrophy and the rise of atmospheric oxygen. *Philosophical Transactions of the Royal Society A: Mathematical, Physical and Engineering Sciences*, *365*(1856), 1867–1888. https://doi.org/10.1098/rsta.2007.2047

Chanton, J. P., Martens, C. S., & Kelley, C. A. (1989). Gas transport from methane saturated, tidal freshwater and wetland sediments. *Limnology and Oceanography*, *34*, 807–819. https://doi.org/10.4319/lo.1989.34.5.0807

Crowe, S. A., Katsev, S., Leslie, K., Sturm, A., Magen, C., Nomosatryo, S., ... Fowle, D. A. (2011). The methane cycle in ferruginous Lake Matano. *Geobiology*, *9*, 61–78. https://doi.org/10.1111/j.1472-4669.2010.00257.x

Crowe, S. A., Paris, G., Katsev, S., Jones, C., Kim, S. T., Zerkle, A. L., ...Canfield, D. E. (2014). Sulfate was a trace constituent of Archean seawater. *Science*, *346*(6210), 735–739.

Daines, S. J., & Lenton, T. M. (2016). The effect of widespread early aerobic marine ecosystems on methane cycling and the Great Oxidation. *Earth and Planetary Science Letters*, *434*, 42–51. https://doi.org/10.1016/j.epsl.2015.11.021

Davidson, T. A., Audet, J., Svenning, J. C., Lauridsen, T. L., Søndergaard, M., Landkildehus, F., … Jeppesen, E. (2015). Eutrophication effects on greenhouse gas fluxes from shallow-lake mesocosms override those of climate warming. *Global Change Biology*, 21, 4449–4463. https://doi.org/10.1111/gcb.13062

Davison, W. (1993). Iron and manganese in lakes. *Earth-Science Reviews*, 34(2), 119–163. https://doi.org/10.1016/0012-8252(93)90029-7

De Wit, P., Pespeni, M. H., Ladner, J. T., Barshis, D. J., Seneca, F., Jaris, H., … Palumbi, S. R. (2012). The simple fool's guide to population genomics via RNA-Seq: An introduction to high-throughput sequencing data analysis. *Molecular Ecology Resources*, 12, 1058–1067. https://doi.org/10.1111/1755-0998.12003

DelSontro, T., Boutet, L., St-Pierre, A., del Giorgio, P. A., & Prairie, Y. T. (2016). Methane ebullition and diffusion from northern ponds and lakes regulated by the interaction between temperature and system productivity. *Limnology and Oceanography*, 61, S62–S77. https://doi.org/10.1002/lno.10335

Dupuis, D., Sprague, E., Docherty, K. M., & Koretsky, C. M. (2019). The influence of road salt on seasonal mixing, redox stratification and methane concentrations in urban kettle lakes. *Science of the Total Environment*, 661, 514–521.

Edgar, R. (2016). UCHIME2: improved chimera prediction for amplicon sequencing. *bioRxiv*. https://doi.org/10.1101/074252.

Eller, G., Känel, L., & Krüger, M. (2005). Cooccurrence of aerobic and anaerobic methane oxidation in the water column of Lake Plußsee. *Applied and Environment Microbiology*, 71(12), 8925–8928.

Etheridge, D. M., Steele, L., Francey, R. J., & Langenfelds, R. L. (1998). Atmospheric methane between 1000 AD and present: Evidence of anthropogenic emissions and climatic variability. *Journal of Geophysical Research: Atmospheres*, 103(D13), 15979–15993.

Fakhraee, M., Crowe, S. A., & Katsev, S. (2018). Sedimentary sulfur isotopes and Neoarchean ocean oxygenation. *Science Advances*, 4(1), e1701835. https://doi.org/10.1126/sciadv.1701835

Fakhraee, M., Hancisse, O., Canfield, D. E., Crowe, S. A., & Katsev, S. (2019). Proterozoic seawater sulfate scarcity and the evolution of ocean–atmosphere chemistry. *Nature Geoscience*, 12(5), 375.

Gohl, D. M., Vangay, P., Garbe, J., MacLean, A., Hauge, A., Becker, A., … Beckman, K. B. (2016). Systematic improvement of amplicon marker gene methods for increased accuracy in microbiome studies. *Nature Biotechnology*, 34, 942–949. https://doi.org/10.1038/nbt.3601

Gorlenko, V. M., Vainstein, M. V., & Chebotarev, E. N. (1980). Bacteria involved in turnover of sulfur and iron metabolism in meromictic Lake Kuznechikha with low sulfate content. *Microbiology*, 49, 653–659.

Goudreault, P. R. (1985). A two-dimensional, finite-difference groundwater flow model of the Minneapolis chain of lakes and surrounding surficial water table aquifer, Doctoral dissertation. University of Minnesota.

Hanson, R. S., & Hanson, T. E. (1996). Methanotrophic bacteria. *Microbiol. Mol. Biol. Rev.*, 60(2), 439–471.

Herndon, E. M., Havig, J. R., Singer, D. M., McCormick, M. L., & Kump, L. R. (2018). Manganese and iron geochemistry in sediments underlying the redox-stratified Fayetteville Green Lake. *Geochimica Et Cosmochimica Acta*, 231, 50–63.

Huttunen, J. T., Alm, J., Liikanen, A., Juutinen, S., Larmola, T., Hammar, T., … Martikainen, P. J. (2003). Fluxes of methane, carbon dioxide and nitrous oxide in boreal lakes and potential anthropogenic effects on the aquatic greenhouse gas emissions. *Chemosphere*, 52, 609–621. https://doi.org/10.1016/S0045-6535(03)00243-1

Jain, A. K., & Juanes, R. (2009). Preferential mode of gas invasion in sediments: Grain-scale mechanistic model of coupled multiphase fluid flow and sediment mechanics. *Journal of Geophysical Research*, 114. https://doi.org/10.1029/2008JB006002

Jones, C., Crowe, S. A., Sturm, A., Leslie, K. L., MacLean, L. C. W., Katsev, S., … Canfield, D. E. (2011). Biogeochemistry of manganese in ferruginous Lake Matano, Indonesia. *Biogeosciences*, 8(10), 2977–2991.

Judd, A., Davies, G., Wilson, J., Holmes, R., Baron, G., & Bryden, I. (1997). Contributions to atmospheric methane by natural seepages on the UK continental shelf. *Marine Geology*, 137, 165–189. https://doi.org/10.1016/S0025-3227(96)00087-4

Juutinen, S., Rantakari, M., Kortelainen, P., Huttunen, J. T., Larmola, T., Alm, J., … Martikainen, P. J. (2009). Methane dynamics in different boreal lake types. *Biogeosciences*, 6, 209–223. https://doi.org/10.5194/bg-6-209-2009

Kasting, J. F. (2005). Methane and climate during the Precambrian era. *Precambrian Research*, 137(3-4), 119–129. https://doi.org/10.1016/j.precamres.2005.03.002

Katsev, S., & Crowe, S. A. (2015). Organic carbon burial efficiencies in sediments: The power law of mineralization revisited. *Geology*, 43(7), 607–610. https://doi.org/10.1130/G36626.1

Katsev, S., Crowe, S. A., Mucci, A., Sundby, B., Nomosatryo, S., Douglas Haffner, G., & Fowle, D. A. (2010). Mixing and its effects on biogeochemistry in the persistently stratified, deep, tropical Lake Matano, Indonesia. *Limnology and Oceanography*, 55, 763–776. https://doi.org/10.4319/lo.2009.55.2.0763

Knauth, L. P. (2005). Temperature and salinity history of the Precambrian ocean: implications for the course of microbial evolution. In N., Noffke (Ed.), *Geobiology: Objectives, concepts, perspectives* (pp. 53-69). Amsterdam, The Netherlands: Elsevier.

Kock, A., Gebhardt, S., & Bange, H. W. (2008). Methane emissions from the upwelling area off Mauritania (NW Africa). *Biogeosciences*, 5, 1119–1125. https://doi.org/10.5194/bg-5-1119-2008

Kozich, J. J., Westcott, S. L., Baxter, N. T., Highlander, S. K., & Schloss, P. D. (2013). Development of a dual-index sequencing strategy and curation pipeline for analyzing amplicon sequence data on the miseq illumina sequencing platform. *Applied and Environment Microbiology*, 79, 5112–5120. https://doi.org/10.1128/AEM.01043-13

Kuntz, L. B., Laakso, T. A., Schrag, D. P., & Crowe, S. A. (2015). Modeling the carbon cycle in Lake Matano. *Geobiology*, 13(5), 454–461. https://doi.org/10.1111/gbi.12141

Laakso, T. A. (2018). Methane multiplication. *Nature Geoscience*, 11(1), 6–7. https://doi.org/10.1038/s41561-017-0043-y

Laakso, T. A., & Schrag, D. P. (2014). Regulation of atmospheric oxygen during the Proterozoic. *Earth and Planetary Science Letters*, 388, 81–91.

Laakso, T. A., & Schrag, D. P. (2019). Methane in the Precambrian atmosphere. *Earth and Planetary Science Letters*, 522, 48–54.

Lambrecht, N., Wittkop, C., Katsev, S., Fakhraee, M., & Swanner, E. (2018). Geochemical characterization of two ferruginous meromictic lakes in the Upper Midwest, USA. *Journal of Geophysical Research: Biogeosciences*, 123(10), 3403–3422. https://doi.org/10.1029/2018JG004587

Lever, M. A., Torti, A., Eickenbusch, P., Michaud, A. B., Šantl-Temkiv, T., & Jørgensen, B. B. (2015). A modular method for the extraction of DNA and RNA, and the separation of DNA pools from diverse environmental sample types. *Frontiers in Microbiology*, 6. https://doi.org/10.3389/fmicb.2015.00476

Lopes, F., Viollier, E., Thiam, A., Michard, G., Abril, G., Groleau, A., … Jézéquel, D. (2011). Biogeochemical modelling of anaerobic vs. aerobic methane oxidation in a meromictic crater lake (Lake Pavin, France). *Applied Geochemistry*, 26, 1919–1932. https://doi.org/10.1016/j.apgeochem.2011.06.021

Lovley, D. R., & Chapelle, F. H. (1995). Deep subsurface microbial processes. *Reviews of Geophysics*, 33(3), 365. https://doi.org/10.1029/95RG01305

McGinnis, D. F., Greinert, J., Artemov, Y., Beaubien, S. E., & Wüest, A. (2006). Fate of rising methane bubbles in stratified waters: How much methane reaches the atmosphere? *Journal of Geophysical Research*, 111(C9). https://doi.org/10.1029/2005JC003183

McGinnis, D. F., & Wuest, A. (2005). *Lake hydrodynamics*. New York, NY: The McGraw Hill Companies.

Mienert, J., Posewang, J., & Baumann, M. (1998). Gas hydrates along the northeastern Atlantic margin: possible hydrate-bound margin instabilities and possible release of methane. *Geological Society, London, Special Publications*, *137*(1), 275–291. https://doi.org/10.1144/gsl.sp.1998.137.01.22

Molofsky, L. J., Richardson, S. D., Gorody, A. W., Baldassare, F., Black, J. A., McHugh, T. E., & Connor, J. A. (2016). Effect of different sampling methodologies on measured methane concentrations in groundwater samples. *Groundwater*, *54*(5), 669–680. https://doi.org/10.1111/gwat.12415

Myrbo, A., Murphy, M., & Stanley, V. (2011). The Minneapolis Chain of Lakes by bicycle: Glacial history, human modifications, and paleolimnology of an urban natural environment, Geological Society of America.

Norði, K. Á., Thamdrup, B., & Schubert, C. J. (2013). Anaerobic oxidation of methane in an iron-rich Danish freshwater lake sediment. *Limnology and Oceanography*, *58*, 546–554. https://doi.org/10.4319/lo.2013.58.2.0546

Olson, S. L., Reinhard, C. T., & Lyons, T. W. (2016). Limited role for methane in the mid-Proterozoic greenhouse. *Proceedings of the National Academy of Sciences*, *113*, 11447–11452. https://doi.org/10.1073/pnas.1608549113

Olson, S. L., Schwieterman, E. W., Reinhard, C. T., & Lyons, T. W. (2018). Earth: Atmospheric evolution of a habitable planet. In H. J., Deeg, J. A., Belmonte (Eds.), *Handbook of exoplanets* (pp 2817–2853). Cham, Switzerland: Springer.

Op den Camp, H. J. M., Islam, T., & Stott, M. B. (2009). Environmental, genomic and taxonomic perspectives on methanotrophic Verrucomicrobia. *Environmental Microbiology Reports*, *1*, 293–306. https://doi.org/10.1111/j.1758-2229.2009.00022.x

Osborn, T. R. (1980). Estimates of the Local Rate of Vertical Diffusion from Dissipation Measurements. *Journal of Physical Oceanography*, *10*, 83–89. https://doi.org/10.1175/1520-0485(1980)010<0083:EOTLRO>2.0.CO;2

Oswald, K., Jegge, C., Tischer, J., Berg, J., Brand, A., Miracle, M. R., … Schubert, C. J. (2016a). Methanotrophy under versatile conditions in the water column of the ferruginous meromictic Lake La Cruz (Spain). *Frontiers in Microbiology*, *7*. https://doi.org/10.3389/fmicb.2016.01762

Oswald, K., Milucka, J., Brand, A., Hach, P., Littmann, S., Wehrli, B., … Schubert, C. J. (2016b). Aerobic gammaproteobacterial methanotrophs mitigate methane emissions from oxic and anoxic lake waters. *Limnology and Oceanography*, *61*, S101–S118. https://doi.org/10.1002/lno.10312

Ozaki, K., Tajika, E., Hong, P. K., Nakagawa, Y., & Reinhard, C. T. (2018). Effects of primitive photosynthesis on Earth's early climate system. *Nature Geoscience*, *11*(1), 55–59. https://doi.org/10.1038/s41561-017-0031-2

Minneapolis Park and Recreation Board. (2013). *Water resources report*. Minneapolis, MN.

Pasche, N., Schmid, M., Vazquez, F., Schubert, C. J., Wüest, A., Kessler, J. D., … Bürgmann, H. (2011). Methane sources and sinks in Lake Kivu. *Journal of Geophysical Research*, *116*(G3). https://doi.org/10.1029/2011JG001690

Pedersen, A. (2017). Package "HMR": Flux estimation with static chamber data. Version 0.4.2.

Planavsky, N. J., McGoldrick, P., Scott, C. T., Li, C., Reinhard, C. T., Kelly, A. E., & Lyons, T. W. (2011). Widespread iron-rich conditions in the mid-Proterozoic ocean. *Nature*, *477*(7365), 448.

Portilho-Ramos, R. C., Cruz, A. P. S., Barbosa, C. F., Rathburn, A. E., Mulitza, S., Venancio, I. M., … Silveira, C. S. (2018). Methane release from the southern Brazilian margin during the last glacial. *Scientific Reports*, *8*(1). https://doi.org/10.1038/s41598-018-24420-0

Posth, N. R., Konhauser, K. O., & Kappler, A. (2013). Microbiological processes in banded iron formation deposition. *Sedimentology*, *60*(7), 1733–1754.

Poulton, S. W., & Canfield, D. E. (2011). Ferruginous conditions: A dominant feature of the ocean through Earth's history. *Elements*, *7*, 107–112. https://doi.org/10.2113/gselements.7.2.107

Pruesse, E., Peplies, J., & Glöckner, F. O. (2012). SINA: Accurate high-throughput multiple sequence alignment of ribosomal RNA genes. *Bioinformatics*, *28*, 1823–1829. https://doi.org/10.1093/bioinformatics/bts252

Reeburgh, W. S. (2007). Oceanic Methane Biogeochemistry. *Chemical Reviews*, *107*, 486–513. https://doi.org/10.1021/cr050362v

Roden, E. E., & Urrutia, M. M. (1999). Ferrous iron removal promotes microbial reduction of crystalline iron(III) oxides. *Environmental Science and Technology*, *33*, 1847–1853. https://doi.org/10.1021/es9809859

Roden, E. E., & Urrutia, M. M. (2002). Influence of biogenic Fe(II) on bacterial crystalline Fe(III) oxide reduction. *Geomicrobiology Journal*, *19*, 209–251. https://doi.org/10.1080/01490450252864280

Roland, F. A., Morana, C., Darchambeau, F., Crowe, S. A., Thamdrup, B., Descy, J. P., & Borges, A. V. (2018). Anaerobic methane oxidation and aerobic methane production in an east African great lake (Lake Kivu). *Journal of Great Lakes Research*, *44*(6), 1183–1193.

Rudd, J. W., & Hamilton, R. D. (1978). Methane cycling in a cutrophic shield lake and its effects on whole lake metabolism 1. *Limnology and Oceanography*, *23*(2), 337–348.

Sanches, L. F., Guenet, B., Marinho, C. C., Barros, N., & de Assis Esteves, F. (2019). Global regulation of methane emission from natural lakes. *Scientific Reports*, *9*(1). https://doi.org/10.1038/s41598-018-36519-5

Savvichev, A. S., Kokryatskaya, N. M., Zabelina, S. A., Rusanov, I. I., Zakharova, E. E., Veslopolova, E. F. … Gorlenko, V. M. (2017). Microbial processes of the carbon and sulfur cycles in an ice-covered, iron-rich meromictic lake Svetloe (Arkhangelsk region, Russia). *Environmental Microbiology*, *19*(2), 659–672. https://doi.org/10.1111/1462-2920.13591

Scandella, B. P., Delwiche, K., Hemond, H. F., & Juanes, R. (2017). Persistence of bubble outlets in soft, methane-generating sediments. *Journal of Geophysical Research: Biogeosciences*, *122*, 1298–1320. https://doi.org/10.1002/2016JG003717

Scandella, B. P., Pillsbury, L., Weber, T., Ruppel, C., Hemond, H. F., & Juanes, R. (2016). Ephemerality of discrete methane vents in lake sediments. *Geophysical Research Letters*, *43*, 4374–4381. https://doi.org/10.1002/2016GL068668

Schindler, D. W. (1978). Factors regulating phytoplankton production and standing crop in the world's freshwaters. *Limnology and Oceanography*, *23*, 478–486. https://doi.org/10.4319/lo.1978.23.3.0478

Schink, B. (1997). Energetics of syntrophic cooperation in methanogenic degradation. *Microbiology and Molecular Biology Reviews*, *61*(2), 262–280.

Schink, B. (2002). Synergistic interactions in the microbial world. *Antonie Van Leeuwenhoek*, *81*(1–4), 257–261.

Schloss, P. D., Westcott, S. L., Ryabin, T., Hall, J. R., Hartmann, M., Hollister, E. B., … Weber, C. F. (2009). Introducing mothur: Open-source, platform-independent, community-supported software for describing and comparing microbial communities. *Applied and Environment Microbiology*, *75*, 7537–7541. https://doi.org/10.1128/AEM.01541-09

Schubert, C. J., Coolen, M. J. L., Neretin, L. N., Schippers, A., Abbas, B., Durisch-Kaiser, E., … Kuypers, M. M. M. (2006). Aerobic and anaerobic methanotrophs in the Black Sea water column. *Environmental Microbiology*, *8*, 1844–1856. https://doi.org/10.1111/j.1462-2920.2006.01079.x

Schubert, C. J., Vazquez, F., Lösekann-Behrens, T., Knittel, K., Tonolla, M., & Boetius, A. (2011). Evidence for anaerobic oxidation of methane in sediments of a freshwater system (Lago di Cadagno). *FEMS Microbiology Ecology*, *76*(1), 26–38.

Shakhova, N., Semiletov, I., Leifer, I., Sergienko, V., Salyuk, A., Kosmach, D., ... Gustafsson, Ö. (2014). Ebullition and storm-induced methane release from the East Siberian Arctic Shelf. *Nature Geoscience*, 7(1), 64–70. https://doi.org/10.1038/ngeo2007

Smith, L. L. (1940). A limnological investigation of a permanently stratified lake in the Huron Mountain region of northern Michigan. *Papers of the Michigan Academy of Science, Arts and Letters*, 26, 3–9.

Stanton, C. L., Reinhard, C. T., Kasting, J. F., Ostrom, N. E., Haslun, J. A., Lyons, T. W., & Glass, J. B. (2018). Nitrous oxide from chemodenitrification: A possible missing link in the Proterozoic greenhouse and the evolution of aerobic respiration. *Geobiology*, 16(6), 597–609. https://doi.org/10.1111/gbi.12311

Stock, D., Leslie, A. G. W., & Walker, J. E. (1999). Molecular architecture of the rotary motor in ATP synthase. *Science*, 286(5445), 1700–1705.

Sturm, A., Fowle, D. A., Jones, C. A., Leslie, K., Nomosatryo, S., Henny, C., ...Crowe, S. A. (2018). Rates and pathways of CH4 oxidation in ferruginous Lake Matano. Indonesia: Geobiology.

Swain, E. (1984). The paucity of blue-green algae in meromictic Brownie Lake: Iron limitation or heavy-metal toxicity? Ph.D. thesis. University of Minnesota.

Taupp, M., Constan, L., & Hallam, S. J. (2010). The biochemistry of anaerobic methane oxidation. Handbook of Hydrocarbon and Lipid. *Microbiology*, 887–907.

Thamdrup, B. (2011). Bacterial manganese and iron reduction in aquatic sediments. In B., Schink (Ed.), *Advances in microbial ecology* (pp 41–84). Boston, MA: Springer.

Ueno, Y., Yamada, K., Yoshida, N., Maruyama, S., & Isozaki, Y. (2006). Evidence from fluid inclusions for microbial methanogenesis in the early Archaean era. *Nature*, 440, 516–519. https://doi.org/10.1038/nature04584

Van Walraven, H. S., Strotmann, H., Schwarz, O., & Rumberg, B. (1996). The H+/ATP coupling ratio of the ATP synthase from thiol-modulated chloroplasts and two cyanobacterial strains is four. *FEBS Letters*, 379(3), 309–313.

Walter, X. A., Picazo, A., Miracle, M. R., Vicente, E., Camacho, A., Aragno, M., & Zopfi, J. (2014). Phototrophic Fe (II)-oxidation in the chemocline of a ferruginous meromictic lake. *Frontiers in Microbiology*, 5, 713.

Wang, Q., Dore, J. E., & McDermott, T. R. (2017). Methylphosphonate metabolism by Pseudomonas sp. populations contributes to the methane oversaturation paradox in an oxic freshwater lake. *Environmental Microbiology*, 19, 2366–2378. https://doi.org/10.1111/1462-2920.13747

Wang, Q., Garrity, G. M., Tiedje, J. M., & Cole, J. R. (2007). Naïve Bayesian classifier for rapid assignment of rRNA sequences into the new bacterial taxonomy. *Applied and Environment Microbiology*, 73, 5261–5267. https://doi.org/10.1128/AEM.00062-07

Weber, H. S., Habicht, K. S., & Thamdrup, B. (2017). Anaerobic methanotrophic archaea of the ANME-2d cluster are active in a low-sulfate, iron-rich freshwater sediment. *Frontiers in Microbiology*, 8. https://doi.org/10.3389/fmicb.2017.00619

Weber, H. S., Thamdrup, B., & Habicht, K. S. (2016). High sulfur isotope fractionation associated with anaerobic oxidation of methane in a low sulfate, iron-rich environment. *Frontiers Earth Science*, 4, 61. https://doi.org/10.3389/feart.2016.00061

Westcott, S. L., & Schloss, P. D. (2017). OptiClust, an improved method for assigning amplicon-based sequence data to operational taxonomic units. *mSphere*, 2(2). https://doi.org/10.1128/mSphereDirect.00073-17

Whiticar, M. J. (1999). Carbon and hydrogen isotope systematics of bacterial formation and oxidation of methane. *Chemical Geology*, 161, 291–314. https://doi.org/10.1016/S0009-2541(99)00092-3

Whiting, G. J., & Chanton, J. P. (1993). Primary production control of methane emission from wetlands. *Nature*, 364, 794–795. https://doi.org/10.1038/364794a0

Wickham, H. (2016). *ggplot2: Elegant graphics for data analysis* (2nd ed.). New York, NY: Springer.

Wirth, T. (1946). Minnesota park system 1883–1944: Retrospective glimpses into the history of the Board of Park Commissioners of Minneapolis, Minnesota, and the city's park, parkway, and playground system. Board of Park, Commissioners.

Wolfe, J. M., & Fournier, G. P. (2018). Horizontal gene transfer constrains the timing of methanogen evolution. *Nature Ecology & Evolution*, 2(5), 897–903. https://doi.org/10.1038/s41559-018-0513-7

Xu, L., Furtaw, M. D., Madsen, R. A., Garcia, R. L., Anderson, D. J., & McDermitt, D. K. (2006). On maintaining pressure equilibrium between a soil CO2 flux chamber and the ambient air. *Journal of Geophysical Research. Atmospheres*, 111, https://doi.org/10.1029/2005JD006435

Yao, M., Henny, C., & Maresca, J. A. (2016). Freshwater bacteria release methane as a by-product of phosphorus acquisition. *Applied and Environment Microbiology*, 82, 6994–7003. https://doi.org/10.1128/AEM.02399-16

SUPPORTING INFORMATION

Additional supporting information may be found online in the Supporting Information section at the end of the article.